



An Optimized Steepest Gradient Based Maximum Power Point Tracking for PV Control Systems

Karima Amara¹, Toufik Bakir², Ali Malek³, Dalila Hocine¹, El-Bay Bourennane², Arezki Fekik¹, and Mustapha Zaouia¹

¹Laboratory of Advanced Technologies of Electrical Engineering (LATAGE), Faculty of Electrical and Computer Engineering, Mouloud Mammeri University of Tizi-Ouzou, Algeria

²Centre de Développement des Energies Renouvelables, BP. 62 Route de l'Observatoire, Bouzareah 16340 Alger, Algérie

³University of Bourgogne, LE2I Laboratory, B.P. 47870, 21078 Dijon Cedex, France
amarakarima140@yahoo.fr.

Abstract : In order to improve the photovoltaic (PV) production, the researchers are interested in developing new methods to reach the Maximum Power Point (MPP) produced by the photovoltaic field to be injected into the utility grid. This article describes a new method called the Optimized Steepest Gradient Method (OSGM), it is based on the first (gradient) and second order (hessian) derivatives of the power function in order to find the best variation of the voltage (V_{pv}) with the calculation of the optimal step allowing the convergence to the tension value (V_{ref}) which ensures the MPP. The mathematical model has been developed and implemented under Matlab/Simulink environment. To analyze Maximum Power Point Tracking (MPPT) algorithm performances, time response, oscillation, overshoot and stability are taken into account. The OSGM is implemented and compared to three others algorithms (one of these algorithm is the ANFIS proposed in previous work). Performances obtained by the proposed algorithm offer faster response, less oscillations around MPP and a low energy loss. In addition, numerical computation of the gradient and the hessian of the power function allow bypassing modeling inaccuracies.

Keywords: MPPT, ANFIS, P&O, MG, OSGM, descent method.

1. Introduction

The major aim of the actual researches in energy field is to find solutions to meet the growing demand of electricity and to reduce its cost. These recent studies explore renewable energies which performances depend on the knowledge of all the elements that constitute renewable energies installations.

Solar energy is considered as one of the most resourceful, fewer toxic process, harmless and noiseless. Like a major systems using solar energy, PV process is of increasing interest in the last years. Unfortunately, the PV system has a disadvantage, which is basically due to its low energy conversion rate caused by the nonlinear characteristic of the photovoltaic generator. To solve such a problem, a MPPT strategy is necessary to reach the MPP of the PV generator under different working conditions.

We consider the case of a nonlinear shape of the power/voltage (P_{pv}/V_{pv}) characteristic that has a single MPP where the system provides its maximum power. To push the system to work at this threshold, numerous researches have been conducted in order to maximize the provided energy by ensuring high-level performances of the PV array. In the case of the sunstroke and the temperature variations, industry utilizes maximum power point tracking (MPPT) algorithms to deliver continuously the greatest possible power to the load.

The MPPT method might be dependent or independent on array model. In the first case, dependent methods are used to generate (offline) a database of parameters (V_{ref} and/or duty cycle) which ensure producing the PV maximum power. To do this, these methods use the

Received: April 25th, 2019. Accepted: December 24th, 2019

DOI: 10.15676/ijeei.2019.11.4.3

collected data from a set of typical power (P_{pv}) curves according to the voltage (V_{pv}) of the PV systems under different irradiances and temperatures conditions. Following these conditions (irradiance and temperature), V_{ref} and/or duty cycle corresponding to the MPP are selected from the (V_{ref} and or/duty cycle) database [1, 2]. In the case of dependent methods, among different intelligent controllers like Artificial Neural Controller (ANN) [3], Adaptive Neuro-Fuzzy Inference System (ANFIS) [4], the Fuzzy Logic Controller (FLC) is the simplest to implement. Recently, FLC received an increasing attention from researchers. This method provides better responses than other conventional controllers [5]-[6]. FLC and ANN methods focus on the nonlinear characteristics of the PV. Some drawbacks are related to rules definition, algorithm complexity and response time to reach the MPP.

In the second case (independent methods), only PV voltage and/or current measurements are used to perform a "real time" tuning of the voltage (V_{pv}) to maximize the power production. These methods have the advantage of being independent from the prior knowledge of the PV array configuration, and thus independent by from the corresponding model parameters. The well-known independent methods are Perturb and Observe (P&O) [7], Hill Climbing (HC) [8], Incremental Conductance (Inc-Cond) [9] and the steepest Gradient Descent [10-13]. P&O is an easy algorithm frequently seen in the industry because of its simplicity; it is based on analyzing the variation of the power ΔP_{pv} which depends on the update of the voltage (V_{pv}) of the PV using a fixed perturbation step. If the ΔP_{pv} is positive the V_{pv} is increased by a given fixed perturbation step, otherwise the V_{pv} is reduced by the same fixed perturbation step and the MPP is gotten when this ΔP is equal to zero. The authors in [14-15] showed that P&O causes wastage of energy because of the oscillations around MPP in the steady state. HC method is based on updating the duty cycle instead of the voltage (in P&O) using a fixed perturbation step as well. In [16-17], the authors showed that HC has a slow response especially under varying weather conditions. Inc-Cond technique is the mostly used by researchers [18]. The perturbation step principal (fixed value) to update voltage by observing the conductance variation is still the same as used in P&O and HC. Basic Inc-Cond algorithm presents some drawbacks when compared to the other methods. In [19- 20], the authors presented a modified Inc-Cond, where the perturbation step is calculated using an adaptive step-size algorithm, while the perturbation step in the basic Inc-Cond is fixed. The modified Inc-Cond is complex and time-consuming when compared to P&O. In [10], MPPT method based on a Gradient method (MG) is used to maximize the power production by updating the voltage (V_{pv}) value. In this case, the V_{pv} variation is calculated using the gradient of the P_{pv} according to V_{pv} and a tuning parameter n . Authors claimed that convergence performances of the algorithm depend on the choice of this parameter. This represents a drawback of this method because of an arbitrary choice of the value of n .

This paper presents a new independent MPPT method called OSGM and based on the gradient (steepest descent) method. We recall that the MPPT methods are based on updating either the Voltage or the duty cycle with a given step value. The accuracy and the efficiency of such methods is directly related to the way to define this step value. Instead of fixed step (P&O methods) or variable step (MG method) using empirical parameter [10], the proposed method allows to update the voltage value in order to reach V_{ref} . The OSGM optimized step is based on a tuning parameter that depends on the second order approximation of the Power function according to the voltage V_{pv} . This method was tested by simulation using MATLAB/SIMULINK under various temperature and sunlight conditions. In addition of new simulations tests, our simulation conditions represent a major part of the previous scenarios discussed in the previous works [7][11][15]. A comparison study between our proposed method and previous methods (P&O, GM and ANFIS based MPPT algorithms) is given in simulation results section.

This paper is organized as follows: Section II presents a brief description of the PV system. Section III is dedicated to the modeling of PV system. In section IV, a comparison between previous MPPT methods and the proposed algorithm is presented. The simulation results and discussion are described in Section V. Finally, a conclusion and some perspectives are given.

2. PV system description

The photovoltaic system contains the SHELL SP75 PV generator connected to DC load via a DC-DC converter (the so-called single stage power conversion). In the case of AC load, DC-AC inverter must be inserted between DC-DC converter and the load (double stage power conversion). The photovoltaic system energy production could exceed the loads needs, the excess energy is then transferred to the electrical network to be consumed by the users of the grid.

The selection of the converters follows different criteria [21]. Among different types of converters, one can site Boost, Buck, or Buck-Boost which are widely used. Converter selection is related to the load needs. Boost converter is used to step up the DC output voltage to be delivered to the load. In the case of AC load, such a converter is used downstream the PV to allow, after DC-AC inverter, delivering a sufficient AC voltage. The Buck converter, in turn, is used to step up the DC current by stepping down the DC voltage following the needs of High-current systems. In the case of system installation which needs different voltage levels, Buck-Boost converter is used to deliver high voltage levels (Boost) and low levels (Buck) by selecting one of the two converters.

In our study case, an AC load is considered which imposes a double-stage PV system. The boost converter is chosen because, in addition to its above-mentioned characteristics, it presents a major advantage which is the possibility to use it in a stand-alone or grid-connected configuration [22- 23]. Concerning inverter (DC-AC) types, there are single-phase and three-phase inverters. These inverters are used in the case of medium and high power need of the load, respectively. We considered in our case a three-phase inverter which is placed between the converter and the AC load (see Figure 1).

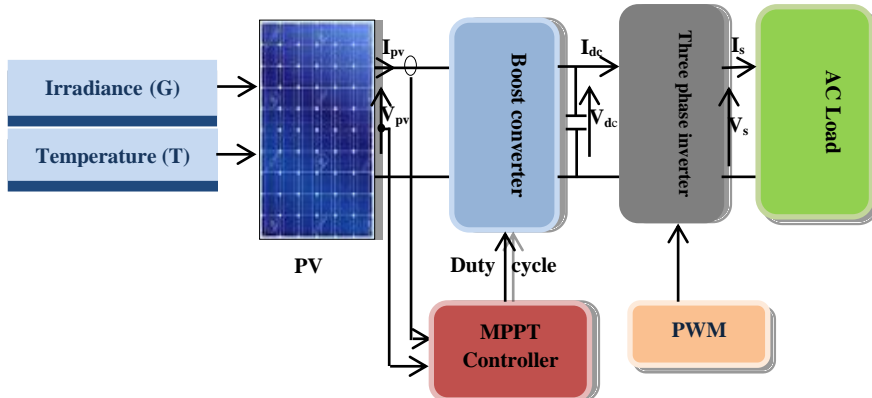


Figure 1. PV system modeling.

PV power production depends on weather conditions (irradiance and temperature). These condition variations induce MPP change. Tracking the MPP is realized by a real time search of the voltage value (V_{ref}) which ensures producing the PV maximum power. When V_{ref} is found using MPPT controller (algorithm), it is imposed to the terminals of the PV ($V_{pv} = V_{ref}$) through the tuning of the duty cycle (D) in the Boot converter (see Figure 2).

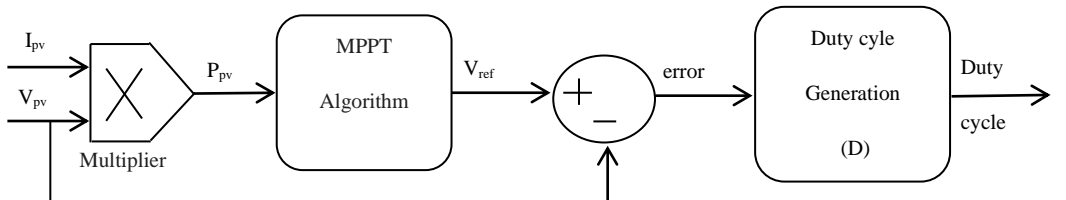


Figure 2. The principle of PV panel control.

Figure 3 represents the illumination and temperature effects on the MPP value and its corresponding voltage V_{ref} . V_{ref} and MPP are directly proportional to the intensity of the illumination G (with $\frac{dV_{ref}}{dG}$ very small). However, V_{ref} and MPP are inversely proportional to the change of the temperature. That is to say when the temperature increase, V_{ref} and MPP decrease and vice versa. PV panel output voltage must follow rapidly V_{ref} changes in order to get MPP. This task is achieved using different MPPT algorithms which performances are measured in terms of tracking speed, oscillations around MPP and stability.

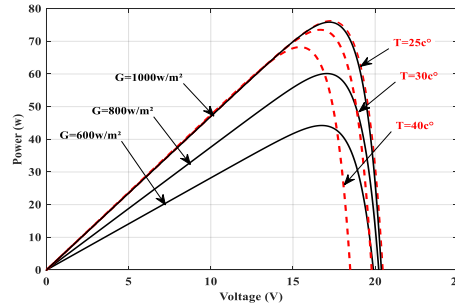


Figure 3. PV power according to the voltage under different conditions (T and G).

3. Mathematical model of the PV system

A. PV panel

In this work, single-diode model of photovoltaic cell is chosen; the traditional I-V characteristic of a solar array is given by the following equations:

$$I_{pv} = I_{ph} - I_0 \left[\exp\left(\frac{V_{pv} + R_s I_{pv}}{V_T}\right) - 1 \right] - \frac{V_{pv} + R_s I_{pv}}{R_{sh}}. \quad (1)$$

$$I_{ph} = (I_{sc} + K_I \Delta T) \frac{G}{G_n}. \quad (2)$$

$$I_0 = I_{rs} \left(\frac{T}{T_{ref}} \right)^3 \left[\exp\left(\frac{-qE_g}{nK} \left(\frac{1}{T} - \frac{1}{T_{ref}} \right)\right) \right]. \quad (3)$$

$$I_{rs} = \frac{I_{sc}}{\exp\left(\frac{V_{oc}}{nN_s V_T}\right) - 1}. \quad (4)$$

Where

$$V_T = \frac{n k T}{q}. \quad (5)$$

V_T : the thermodynamic potential (J/C).

n: the ideality factor of the solar cell.

G: (the irradiance (W/m^2)).

K: the Boltzmann's constant ($1.3805 \cdot 10^{-23} J/K$).

q: the electron charge ($1.6 \cdot 10^{-19} C$).

T: the operating cell temperature (K).

T_{ref} : the reference temperature ($T=283K$).

ΔT : the difference of $T-T_{ref}$ (K).

I_{pv} , V_{pv} , P_{pv} : the cell output current (A), voltage (V) and power (W), respectively.

I_{ph} : the light-generated current (A), which is directly proportional to G.

I_{sc} , V_{oc} : the short circuit courant (A) and the open circuit voltage (V).

K_I : the temperature coefficients of the short-circuit current (A/K).

I_0 : the cell reverse saturation current (A).

N_s : the number of cells connected in series.

R_s , R_{sh} : the series and shunt resistor (Ω), respectively.

E_g : the physical band gap energy (eV), (1.12 eV for Si).

Table 1. The SHELL SP75 PV module parameters.

Module parameters	Values
Power at MPP: P_{\max}	$P_{\max}=75 \text{ W}$
Open circuit voltage: V_{oc}	$V_{oc}=21.7 \text{ V}$
Short current circuit: I_{sc}	$I_{sc}=4.8 \text{ A}$
Voltage at MPP: V_{mpp}	$V_{mpp}=17 \text{ V}$
Current at MPP: I_{mpp}	$I_{mpp}=4.4 \text{ A}$

B. The boost converter DC-DC

Figure 4 shows a typical Boost converter which contains two electrical storage elements (inductor L and capacitor C). Following the command value u , the switch state commutes between ON mode ($t \in [0, D*T]$) and OFF mode ($t \in [D*T, (1-D)T]$), D being the duty cycle. The Boost converter takes then two configurations which are represented by two different models (based on differential equations):

Switch ON ($u=1$)

$$V_{pv} = L \frac{dI_L}{dt} \quad (6)$$

$$0 = C \frac{dV_{dc}}{dt} + I_{dc} \quad (7)$$

Switch OFF ($u=0$)

$$V_{pv} = L \frac{dI_L}{dt} + V_{dc} \quad (8)$$

$$I_L = C \frac{dV_{dc}}{dt} + I_{dc} \quad (9)$$

The above mentioned two models of the converter can be gathered in the unique equations system:

$$V_{pv} = L \frac{dI_L}{dt} + (1 - u)V_{dc} \quad (10)$$

$$I_L(1 - u) = C \frac{dV_{dc}}{dt} + I_{dc} \quad (11)$$

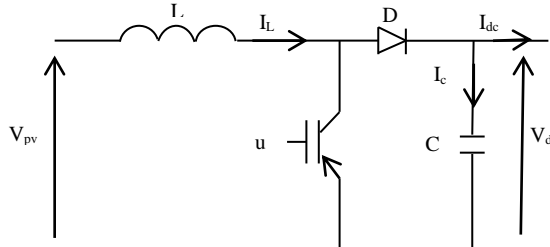


Figure 4. Boost converter

Replacing the variable u by its average value D (duty cycle) over a period $T=1/f$. That is to say the duty cycle D ($D = T_{ON} / T$), we can get the average model [24]:

$$V_{pvm} = \frac{1}{L} \frac{dI_{lm}}{dt} + (1 - D)V_{dcm} \quad (12)$$

$$I_{lm}(1 - D) = \frac{1}{C} \frac{dV_{dcm}}{dt} + I_{dcm} \quad (13)$$

Where V_{pvm} and V_{dcm} are the input and output average voltages values respectively. I_{lm} and I_{dcm} are the inductor average current and the output average current values respectively. The relationship of the mean values between input and output voltage is given by

$$V_{dcm} = \frac{1}{(1-D)} V_{pvm} \quad (14)$$

C. Modeling of three-phase inverter DC-AC

The power circuit is usually built up from Insulated Gate Bipolar Transistor (IGBT) switches and contains a bridge of six power transistors with anti-parallel diodes (see Figure5). These six transistors are switching in a predesigned sequence by sending a signal to their gate pins. This signal is generated by the control circuit Pulse Width Modulation (PWM).

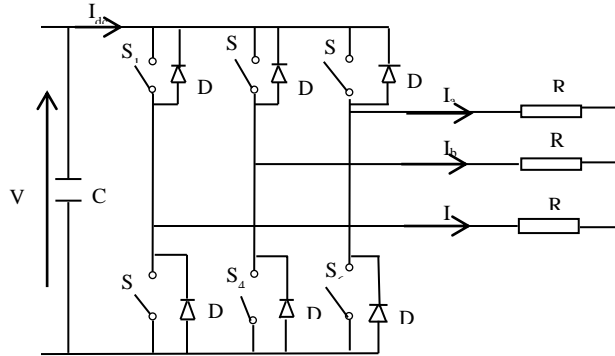


Figure 5. Electrical diagram of the inverter and load

In our case we choose the three-phase inverter, the composed voltages V_{ab} , V_{bc} , V_{ca} are obtained from these relationships:

$$\begin{cases} V_{ab} = V_{ao} + V_{bo} = V_{ao} - V_{bo} \\ V_{bc} = V_{bo} + V_{co} = V_{bo} - V_{co}, \\ V_{ca} = V_{co} + V_{oa} = V_{co} - V_{ao} \end{cases} \quad (15)$$

With: V_{ao} , V_{bo} and V_{co} are the voltages at the input of the inverter (continuous voltages) and the point "O" is the reference point. These voltages are given by

$$\begin{cases} V_{ao} = V_{an} + V_{no} \\ V_{bo} = V_{bn} + V_{no}. \\ V_{co} = V_{cn} + V_{no} \end{cases} \quad (16)$$

With V_{an} , V_{bn} , V_{cn} are the phase voltages of the load (inverter output) and V_{no} is the neutral voltage of the load with respect to the "O" point. [25]. It has been assumed that the load is balanced:

$$V_{an} + V_{bn} + V_{cn} = 0. \quad (17)$$

Replacing (17) in (16) yields:

$$V_{no} = \frac{1}{3} \times (V_{ao} + V_{bo} + V_{co}). \quad (18)$$

And (18) in (16) we will have:

$$\begin{cases} V_{an} = \frac{1}{3} \times (2V_{ao} - V_{bo} - V_{co}) \\ V_{bn} = \frac{1}{3} \times (2V_{bo} - V_{ao} - V_{co}). \\ V_{cn} = \frac{1}{3} \times (2V_{co} - V_{ao} - V_{bo}) \end{cases} \quad (19)$$

If we assume that:

$$\begin{cases} V_{ao} = V_{dc} \times S_a \\ V_{bo} = V_{dc} \times S_b. \\ V_{co} = V_{dc} \times S_c \end{cases} \quad (20)$$

Where the S_i ($i=a, b, c$) is the switch state:

$S_i = 1$ if K is closed.

$S_i = 0$ if K is open.

Then:

$$\begin{bmatrix} V_{ar} \\ V_{br} \\ V_{cr} \end{bmatrix} = \frac{V_{dc}}{3} \begin{bmatrix} 2 & -1 & -1 \\ -1 & 2 & -1 \\ -1 & -1 & 2 \end{bmatrix} \cdot \begin{bmatrix} S_a \\ S_b \\ S_c \end{bmatrix} \quad (21)$$

The modulated current (input current (I_{dc})) by the inverter is given by:

$$I_{dc} = S_a \times I_a + S_b \times I_b + S_c \times I_c \quad (22)$$

4. MPPT techniques

As abovementioned, we present P&O and GM MPPT algorithms, we present also ANFIS based MPPT algorithm which was proposed in our previous work [4]. Finally we proposed our new MPPT algorithm (OSGM).

A. Conventional perturb and observe (P&O) description

The principal of the algorithm P&O is given by Figure 6, it consists of comparing the power- to-voltage ratio to zero ($\frac{\Delta P_{pvk}}{\Delta V_{pvk}}$) to update the voltage value in order to reach the MPP:

$$V_{ref_{k+1}} = V_{ref_k} \pm step. \quad (23)$$

With **step** is constant in the conventional P&O. If the ratio $\frac{\Delta P_{pvk}}{\Delta V_{pvk}}$ is positive, the V_{ref_k} is increased by a given fixed perturbation **step** in order to reach the Maximum Power Point (MPP) production, else the V_{ref_k} is decreased by the same given fixed perturbation **step**. The MPP is reached when this ratio is very close to zero.

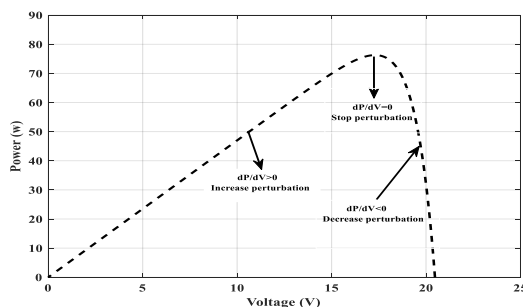


Figure 6. Principal of perturbation

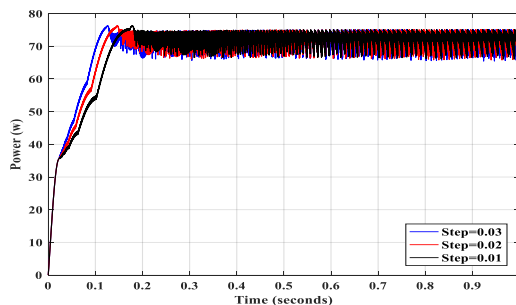


Figure 7. Power tracking curve

For instance, Figure 7 shows the MPPT results using P&O algorithm under standard weather conditions (irradiance $G=1000W/m^2$, $T=25C^\circ$) and using three fixed step values (0.01,0.02,0.03).

These curves exhibit oscillations of the PV power around the MPP which are caused by P&O algorithm, inducing by the way energy wasting of the PV generator. The simulation results show that MPPT efficiency is related to the step value; following small/large step value, the algorithm exhibits a low/high convergence speed and small/large oscillations, respectively. That is to say, the step should be large when the operating point is far from the MPP in order to speed up the monitoring process, while the step should be small when the operating point is close to the MPP to reduce oscillations and tracking error. In this way the following algorithm uses an adaptive step to update the voltage value.

B. Gradient descent Method (GM)

This method is actually a modified gradient method (steepest descent method), which can be used to solve nonlinear problems. This algorithm was used as an MPPT method [10]. The

V_{ref_k} updating value depends on $\frac{\Delta P_{pvk}}{\Delta V_{pvk}}$ and n (perturbing coefficient):

$$V_{ref_{k+1}} = V_{ref_k} + K \frac{\Delta P_{pvk}}{\Delta V_{pvk}} \left(e^{\left| \frac{\Delta P_{pvk}}{\Delta V_{pvk}} \right|} - 1 \right)^n. \quad (24)$$

Where

$$step_k = K \frac{\Delta P_{pvk}}{\Delta V_{pvk}} \left(e^{\left| \frac{\Delta P_{pvk}}{\Delta V_{pvk}} \right|} - 1 \right)^n. \quad (25)$$

And K is a constant parameter. If $\frac{\Delta P_{pvk}}{\Delta V_{pvk}} = 0$ (ideal case), the updating value is equal to zero which means that $V_{ref_{k+1}} = V_{ref_k}$ (the MPP is reached). However $\frac{\Delta P_{pvk}}{\Delta V_{pvk}} = \varepsilon$ in

practice (close to zero), which make this algorithm oscillating around the MPP because of the empirical value of n. This method has three drawbacks:

- A fast step change at the beginning tracking process ($P_{pv_{max}} = P_{pv}(0) = I_{sc}$) [10], which affect the system stability.
- Constant value of the K which can reduce the tracking efficiency.
- Empirical choose of perturbing coefficient n when $(e^{\left| \frac{\Delta P_{pv}}{\Delta V_{pv}} \right|} - 1) > 1$, where $0 < n < 1$.

These two previous MPPT algorithms present different drawbacks. P&O step value is fixed which causes a loss of energy. In the case of MG MPPT, the step value depends on empirical parameters (K and n). These chosen K and n parameters could not be the best ones to get the best method performances. To overcome these problems in previous MPPT methods, we propose in this work an MPPT method (OSGM method) where $step_k$ is based on the gradient (steepest descent) method. $step_k$ depends also on a parameter α which optimal value α^* (allowing to get the optimal update of V_{pv}) is based on the first and the second derivatives of P_{pv} (gradient and hessian, respectively). Before giving details of OSGM method, let's introduce our previous proposed algorithm (ANFIS-based MPPT method) which is a dependent method [4]. P&O, GM, ANFIS-based MPPT and OSGM methods will be compared in simulation results section.

C. The ANFIS-MPPT

The Fuzzy Adaptation Inference System (ANFIS) combines the Artificial Neural Networks ANN and Fuzzy Logic Control FLC functions in a single block. ANFIS gives the advantage of using the ANN to optimize the limits of the membership function (MFs) of the Fuzzy Inference System FIS. From a database, ANFIS-based MPPT allow generating a model relating the working conditions and V_{ref} which ensures the MPP.

In the case of 2 inputs (see Figure8), the architecture of ANFIS-based MPPT has five layers (fixed and adaptive layers, (see [4])).

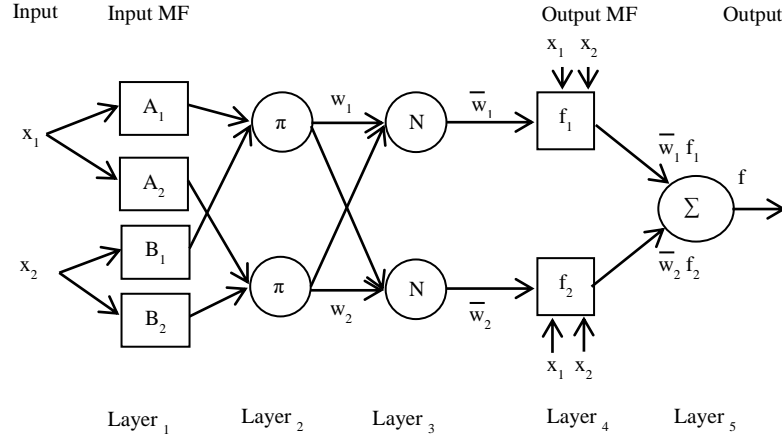


Figure 8. The ANFIS architecture

The first layer L^1 gives the membership functions (MFs) of the 2 inputs signals x_1 and x_2 ($\mu_{MF_{ij}}$) which are the variation of the irradiance (G) and the PV voltage (V_{pv}), respectively:

$$L^1_{ij} = \mu_{MF_{ij}}(x_i), i = 1, 2, j = 1, 2. \quad (26)$$

With: $MF_{1,1}=A_1$, $MF_{1,2}=A_2$, $MF_{2,1}=B_1$, $MF_{2,2}=B_2$.

The second layer L^2 calculates the firing strengths of each rule via multiplying the all incoming signals:

$$L^2_j = W_j = \prod_{i=1}^2 \mu_{MF_j}(x_i), j = 1, 2. \quad (27)$$

The third layer L^3 calculates the ratio of the i^{th} rule's firing strength to the sum of all rule's firing strength:

$$L^3_j = \bar{W}_j = \frac{W_j}{W_1 + W_2}, j = 1, 2. \quad (28)$$

The fourth layer L^4 is simply the product of the normalized firing strength and a first order polynomial:

$$L^4_j = \bar{W}_j f_j = \bar{W}_j (p_j x_1 + q_j x_2 + r_j), j = 1, 2. \quad (29)$$

Where f_j is the first order Takagi-Sugeno's type [26-28].

The last layer (fifth layer) L^5 calculates the summation of all incoming signals:

$$L^5 = \sum_{j=1}^2 \bar{W}_j f_j \quad (30)$$

D. Proposed method OSGM

This proposed MPPT method (iterative algorithm) is based on the steepest descent method which can be used in the case of minimizing or maximizing (our study case) a cost function

$F(X_k)$ by optimizing the parameters vector X_k . In the following, we recall in the general case the fundamentals of this method (based on the first order Taylor approximation) and we give the expression of the optimized updating step_k (based on the second order Taylor approximation). Let be the cost function $F(X_k)$ at iteration k (X_k is the vector to be optimized). The first order Taylor approximation of $F(X_k)$ in the neighborhood of X_k is;

$$F(X_k) + \Delta F(X_k) = F(X_k + \delta_k). \quad (31)$$

$$F(X_{k+1}) = F(X_k) + g^T(X_k)\delta_k = F(X_k) + \delta_k F(X_k). \quad (32)$$

With

$$g_k = g(X_k) = \nabla(F(X_k)). \quad (33)$$

And

$$X_k \in \mathbb{R}^{n \times 1}, g(X_k) \in \mathbb{R}^{n \times 1}, \delta_k \in \mathbb{R}^{n \times 1}.$$

Then:

$$\Delta F(X_k) = \sum_{i=1}^n g_i \delta_i = \|g_k\| \|\delta_k\| \cos \theta_k. \quad (34)$$

In the case of maximizing $F(X_k)$ (maximizing $F(X_k) = P_{pv}$ in our case, $X_k = V_{ref_k}$), the maximum increase of $F(X_k)$ is obtained when.

$$\theta_k = 0 \Rightarrow \delta_k = g_k. \quad (35)$$

Where:

δ_k is the steepest descent direction.

In practice (numerical computation), δ_k does not always point to X^* (the optimized value of X_k). A tuning parameter α (α is positive) is then necessary to ensure the convergence of the algorithm to the X^* solution. Let's consider the case of maximizing $F(X_k)$, then:

$$X_{k+1} = X_k + \alpha g_k, \quad \alpha > 0. \quad (36)$$

An optimal choice of α could be achieved using the second order approximation of $F(X_{k+1})$.

$$F(X_k + \delta_k) \approx F(X_k) + \alpha g_k^T g_k + \frac{1}{2} \alpha^2 g_k^T H_k g_k. \quad (37)$$

Where:

$$H_k = \nabla^2 F(X_k). \quad (38)$$

If the Hessian of $F(X_k)$ is accessible, α^* that minimizes $F(X_k)$ can be determined analytically:

$$\frac{dF(X_k + \alpha g_k)}{d\alpha} = g_k^T g_k + \alpha g_k^T H_k \delta_k. \quad (39)$$

$$\frac{dF(X_k + \alpha g_k)}{d\alpha} = 0 \Rightarrow \alpha^* = -\frac{g_k^T g_k}{g_k^T H_k g_k}. \quad (40)$$

In the general case ($X \in \mathbb{R}^{n \times 1}$), $H \in \mathbb{R}^{n \times n}$ is a negative definite matrix when $F(X_k)$ is a concave function, then $\alpha > 0$ (see eq.36).

Then:

$$X_{k+1} = X_k - \frac{g_k^T g_k}{g_k^T H(X_k) g_k} g_k. \quad (41)$$

In this study case $X_k = V_{pv_k}$ (voltage) is a scalar (one parameter). The power function $P_{pv_k} = F(V_{ref_k})$ is a concave function (with a maximum value MPP). g_k and H_k of $P_{pv_k}(V_{pv_k})$ are then the first and the second derivative of the power function, respectively. Using $P_{pv_k}(V_{pv_k})$ expression based on current and voltage values.

$$P_{pv_k} = V_{pv_k} I_{ph} - V_{pv_k} I_0 \left[\exp\left(\frac{V_{pv_k}}{V_T}\right) - 1 \right]. \quad (42)$$

Analytical expressions of g_k and H_k are given by:

$$g_k = \frac{dP_{pv_k}}{dV_{pv_k}} = I_{ph} - I_0 \left[\exp\left(\frac{V_{pv_k}}{V_T}\right) - 1 \right] + \frac{I_0 V_{pv_k}}{V_T} \exp\left(\frac{V_{pv_k}}{V_T}\right). \quad (43)$$

$$H_k = \frac{d^2 P_{pv_k}}{dV_{pv_k}^2} = \frac{I_0}{V_T} \left[2 \exp\left(\frac{V_{pv_k}}{V_T}\right) - \frac{V_{pv_k}}{V_T} \exp\left(\frac{V_{pv_k}}{V_T}\right) \right]. \quad (44)$$

These derivatives depend on circuit components values which can be poorly known because of equipment aging for instance. For this, a numerical gradient and hessian values could be calculated as following:

$$g_k = \frac{P_{pv_k} - P_{pv_{k-1}}}{V_{pv_k} - V_{pv_{k-1}}}. \quad (45)$$

$$H_k = \frac{g_k - g_{k-1}}{V_{pv_k} - V_{pv_{k-1}}}. \quad (46)$$

And:

$$V_{ref_{k+1}} = V_{ref_k} - \frac{g_k^T (V_{ref_k}) g_k (V_{ref_k})}{g_k^T (V_{ref_k}) H (V_k) g_k (V_{ref_k})} g_k (V_{ref_k}). \quad (47)$$

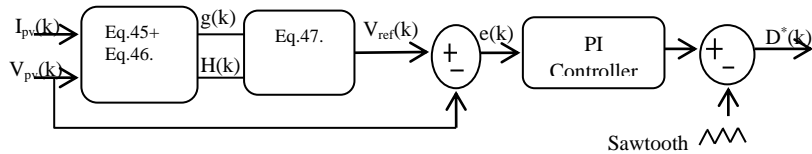


Figure 9. Schematic diagram of the proposed method based on OSGM.

5. Simulation Results

Using the above detailed model, simulation results were carried out with the conventional P&O, GM, ANFIS algorithms and the proposed OSGM based MPPT for evaluation and comparison analysis.

To show the efficiency of the proposed independent method OSGM:

A firstly test compares the OSGM with two independent methods which are the conventional P&O and the GM algorithms under fast and slow variation of irradiation (G) and temperature (T).

A seconds test compares the OSGM with the intelligent dependent method which is ANFIS (this method was tested in our previous work [4]) under fast and slow variation of irradiation (G) and temperature (T). The simulations are performed under the following test conditions:

- Constant temperature ($T=25^\circ C$) and constant solar irradiation ($G=1000W/m^2$).
- Constant temperature ($T=25^\circ C$) and slow change of the G.
- Constant temperature ($T=25^\circ C$) and fast change of the irradiance from ($G=600W/m^2$) to ($G=1000W/m^2$).
- Constant irradiation ($G=1000W/m^2$) with a slow change of temperature (T).
- Constant of the solar irradiation ($G=1000 W/m^2$) with a fast change of temperature (T) from $T=24^\circ C$ to $T=50^\circ C$.

A third test compares the OSGM with three methods which are P&O, GM and ANFIS methods following the conditions given in [11], [31].

The main important parameters to analyze performance of each MPPT algorithm are oscillation, overshoot and stability in steady state and tracking speed.

A. First test: the OSGM, the conventional P&O and GM based MPPT

Figure 10 represents the simulation results of the three MPPT methods (OSGM, GM and P&O) under constant sunlight test (a): constant temperature (see Figure10 (1)). The best performances are obtained when using the OSGM with an output power close to 75 W. Indeed, considering the response time, P&O represents the most degraded algorithm when compared to the time response of the GM and the OSGM which response times are very close. However, OSGM exhibit the best performances in steady state with a very small oscillation when compared to the two other methods (P&O and GM) (see Figure10 (2)).

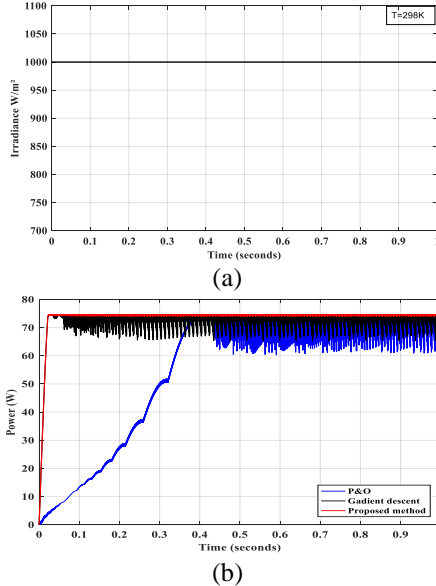


Figure 10. (a) the Standard Test Conditions (STC), (b) Power supply under STC

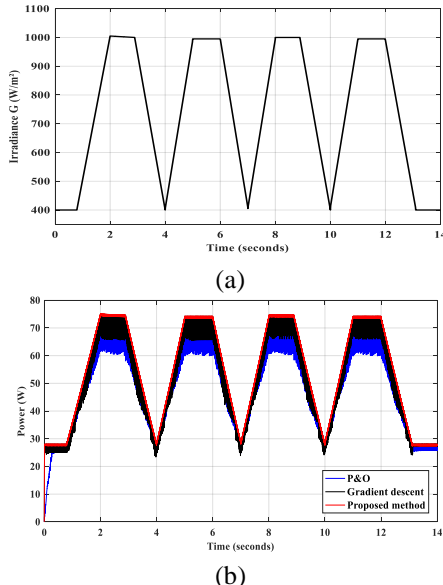


Figure 11. (a) the slow change of the irradiance levels (G),
(b) The power supply under slow change between different levels of G

Figure 11 (a) represents the test (b) which corresponds to a slow change of the irradiance from the $G=400W/m^2$ to $G=1000W/m^2$.

Figure 11 (b) shows the simulation results of the three MPPT methods in the case of the test (b). As expected, the output power tracking with the OSGM algorithm is the best one in terms of power value (highest output power) and stability (very small oscillations).

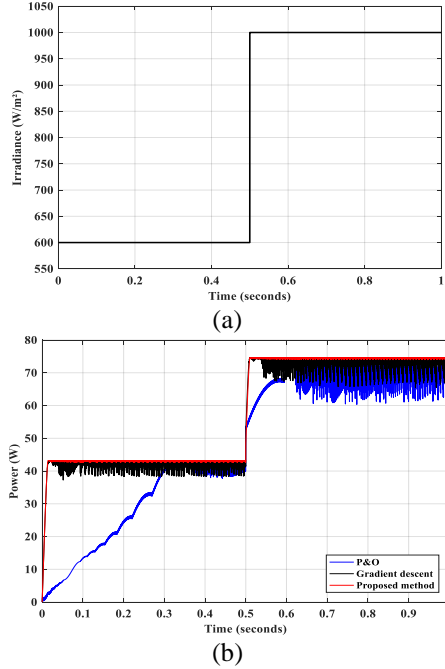


Figure 12. (a) the fast change of irradiance from $G=600W/m^2$ to $G=1000W/m^2$,
(b) Power variation under fast change of irradiance (G).

Figure 12 (a) represents the fast change of irradiance from $600 W/m^2$ to $1000 W/m^2$ (test (c)), The OSGM gives an MPP of 43W for $600W/m^2$ and 74.5W for $1000 W/m^2$, 74.5 W is very close to the maximum power of the used PV panel (the SHELL SP75 PV panel) (see Figure 12 (2)), when P&O and GM algorithms are oscillating around smaller MPP values. Also the small oscillations of the OSGM algorithm (with a MPP of 74.5 W) are due to resistances in the DC-DC module which cause a power loss.

Also, despite the power loss due to resistances in the DC-DC module, small oscillations of the OSGM algorithm (with a MPP of 74.5 W) are observed, when the other algorithms exhibit a very large oscillations, which shows the robustness of the OSGM Algorithm with respect to circuit components.

The Figure 13 (1) represents the test (d) which is the slow change of the temperature from $T=24^\circ C$ to $T=50^\circ C$. As shown in Figure 13 (2), the power is inversely proportional to the temperature (T), that is to say when the T increases the maximum power produced decreases and vice versa. The MPP tracking when using the OSGM is still better compared to both methods (P&O and GM).

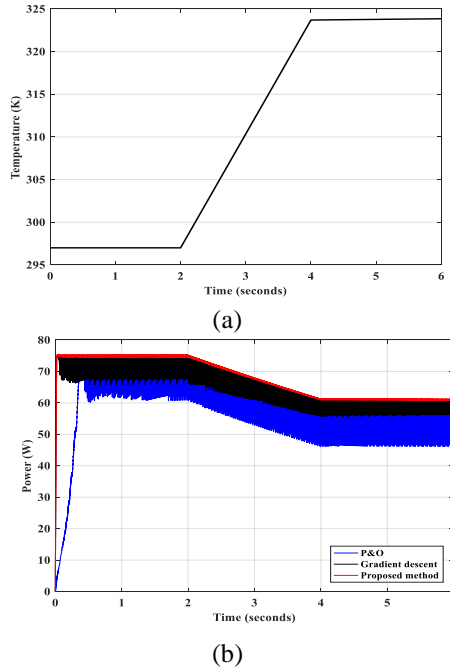


Figure 13. (a) the slow change of the temperature (T), (b) PV power change under slow variation of the temperature (T).

The Figure 14 (a) represents the fast change of the temperature from $T=24^{\circ}\text{C}$ to $T=50^{\circ}\text{C}$ (test (e)). Despite the sudden change in temperature, the OSGM method remains the most reliable in terms of monitoring (see Figure 14 (b)).

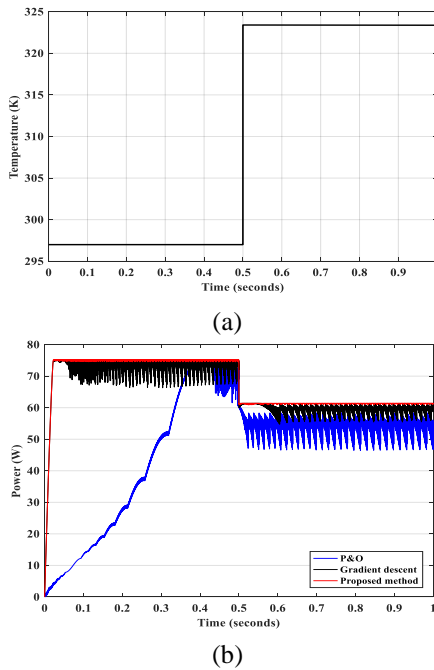


Figure 14. (a) the fast change of the temperature from $T=24^{\circ}\text{C}$ to $T=50^{\circ}\text{C}$,
(b) Power under fast change of the temperature (T).

To check the effectiveness of the independent proposed method (OSGM) compared to the dependent method, a comparison of the OSGM with another intelligent method which is an Adaptive Fuzzy-Neural Inference System ANFIS is presented below.

B. Second test: the OSGM and ANFIS based MPPT

The Figure 15 (a) gives the simulation results of the proposed OSGM and the intelligent ANFIS (in the case of the test (a)), from these simulation results, OSGM exhibits better performances in term of response time and stability when compared to ANFIS method.

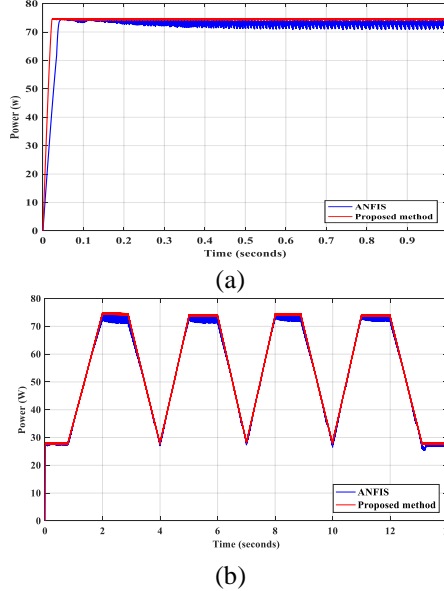


Figure 15. (a) The power supplied under Standard test conditions,
(b) the power supplied under slow change of the G.

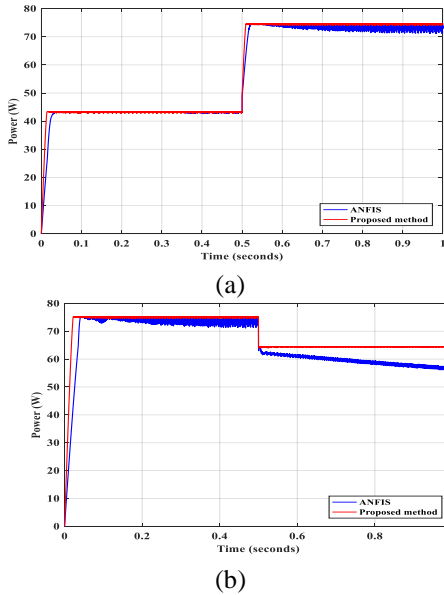


Figure 16. (a) PV power provided under the sudden change of G,
(b) Power supplying under the fast change of T.

Under slow change of the irradiance (in the case of test (b)), the two algorithms give a high yield of the power panel supply, (see Figure 15 (b)) with better stability of OSGM in the case of constant irradiance.

The photovoltaic power transfer from the source to the load remains optimal even in the sudden change (test (c)) of illumination using the two algorithms (ANFIS and OSGM) as shown in the Figure 16 (a).

The power supply to the loads with the OSGM is very good even when the temperature changes rapidly (test (e)), but ANFIS fails under fast change of temperature as shown in the Figure 16 (b).

C. The third test: the OSGM, GM, P&O and ANFIS methods following the conditions given in [31], [11]:

In [11, 15, 29, 30] and [33], authors used irradiance conditions of (500W/m² to 1000W/m²), 400W/m² to 1000W/m² and 1000 W/m² to 400 W/m² and 1000W/m² to 400W/m², respectively. In [31-36] and [7] authors evaluate their control MPPT under change of irradiance from 600W/m² to 1000W/m², 500W/m² to 1000 W/m², they used three different tests like; G = 493 W/m² and T = 294K, G = 858 W/m² and T = 299K and finally G = 493W/m² and T = 292 K, the change of irradiance from G=1000W/m² to G=900W/m², they used the irradiance change from G=600W/m² to G=1000W/m² and 300W/m² to 600W/m² and 1000W/m² and the temperature increases from T = 300K to T = 330K, respectively.

Our proposed MPPT method is tested following the most scenarios (temperature and irradiance ranges and variations) of the previous works as abovementioned. In addition, we added dynamic irradiance changes (triangular shape variation) which are the most complicated tests to check the effectiveness of our proposed method.

We reproduce the same conditions of irradiance (G) and temperature (T) already used in [31] to test the efficiency of our OSGM method (see Figure 17 (a), (b)). The response with OSGM is very stable and fast compared to the other methods (see Figure 18).

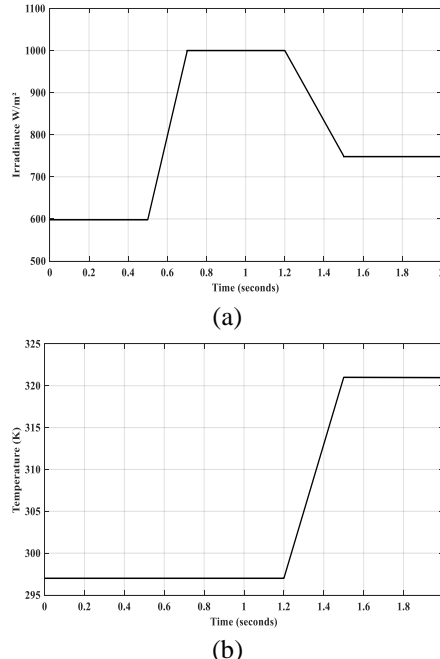


Figure 17. (a) the change of irradiance levels according to [31], (b) the temperature (T) change according to [31].

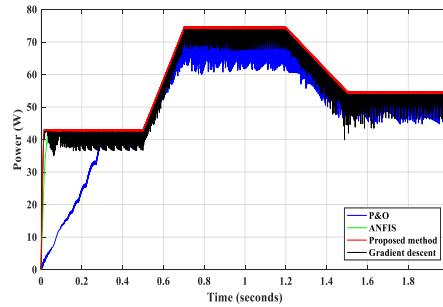
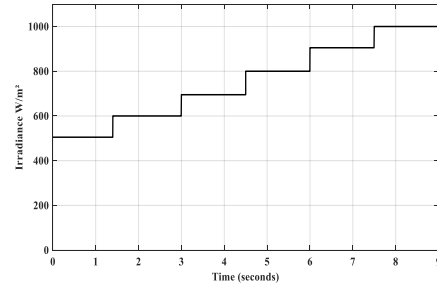


Figure 18. the PV power supplying according to [31] conditions of G and T.

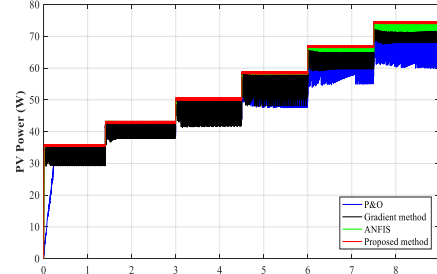
In this case we tested our OSGM method according to the irradiance levels given in [11]. As shown in Figure 19 (a) the PV generator provides its maximum power at each level of irradiance with the four methods. But we notice better stability and speed response with the OSGM method (see Figure 19 (b)).

As indicated in Figure 20 (a), at each irradiance level change, the MPPT commands adjusted the PV voltage at the reference value despite the presence of jumps at each change. The voltage jumps with OSGM method are small compared to jumps with other methods which give a stable PV voltage.

The comparison tracking with the four methods is given in Figure 20 (b) the P&O and GM methods track the reference voltage what corresponds to MPP and they oscillate around this point. The OSGM and ANFIS methods track the reference voltage and tried to stabilize in this point which reduces the oscillations around the MPP, but the Tracking with OSGM is better than the ANFIS MPPT Tracking.



(a)



(b)

Figure 19. (a) the variation of irradiance according to [11],
 (b) The PV power under [11] conditions

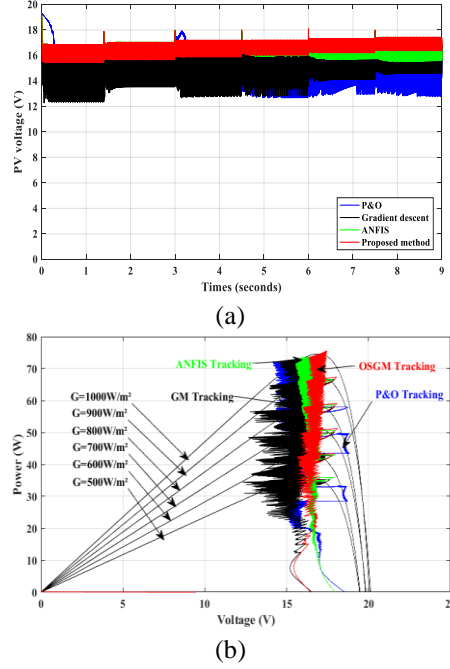


Figure 20. (a) the variations of PV voltage following the conditions in [11],
(b) the comparison Tracking with the four methods.

Table 2. Comparison of tracking behavior of OSGMS with P&O, GM and ANFIS at STC

MPPT Techniques	P_{mpp} (Watts)	V_{mpp} (Volts)	Time response (Seconds)	The larger of oscillations
Actual	75.00	17.00	-----	-----
OSGM	74.50	16.80	0.03 (very Fast)	Small
ANFIS	74.45	16.78	0.05 (Fast)	Small
GM	74.30	16.00	0.09 (Fast)	large
P&O	72.80	15.60	0.40 (Slow)	Very large

Table 3. MPP calculated at different environmental conditions

G (Watts/m ²)	V_{mpp} (Volts)	I_{mpp} (Amps)	P_{mpp} (Watts)
1000	16.80	4.44	74.50
900	16.49	4.10	67.78
800	16.10	3.69	59.88
700	16.00	3.18	51.80
600	15.89	2.79	44.80
500	15.70	2.35	37.19

MPP parameters calculated at different levels of irradiance are listed in Table.III. From this Table and the simulation results, it is show that the performances of dynamic state and steady state have better improvement when using the OSGM algorithm.

6. Conclusion

A novel MPPT-based OSGM algorithm for the PV system has been presented. A comparison was made between the independent conventional P&O, GM methods and the independent proposed OSGM method, then between the OSGM and the dependent intelligent ANFIS method. All these algorithms were detailed, simulated and implemented under

Matlab/Simulink, and tested under irradiation and temperature variations (fast and slow changes).

From the simulation results, clearly the OSGM method reaches quickly (small response time) and accurately (stability) the MPP with very small oscillations of the power around the steady-state, decreasing the energy losses and improving the energy harvesting to ensure the good use of PV system. Indeed, P&O algorithm exhibits constant oscillation around the MPP due to the fixed step perturbation and thus generating considerable energy losses, GM algorithm presents also oscillations around the MPP because the perturbing coefficient based on empirical parameters, ANFIS algorithm exhibits good response under irradiance variation but it fails under fast changes of the temperature. Additionally, response times of these three algorithms are very large when compared to OSGM response time, which is the main advantage of this proposed method.

We emphasize that the OSGM is the algorithm recommended for the implementation in real systems. This is due to V_{ref} update expression which depends on first and second order derivatives of the PV power. These derivatives could be performed in a numerical way, which eliminates modelling errors and has robust technique. In the future work, we plan to implement this proposed method on a real PV panel, and to develop a control strategy of a three phases in order to synchronize the PV production with the utility grid.

7. References

- [1] Khatib, Tamer TN, et al. An improved indirect maximum power point tracking method for standalone photovoltaic systems. *Proceedings of the 9th WSEAS International Conference on Applications of Electrical Engineering, Selangor, Malaysia*. 2010.
- [2] Jain, Sandeep, and Vivek Agarwal. Comparison of the performance of maximum power point tracking schemes applied to single-stage grid-connected photovoltaic systems. *IET Electric Power Applications* Vol 1(5), pp 753-762, 2007.
- [3] Chekired, F, et al. Implementation of a MPPT fuzzy controller for photovoltaic systems on FPGA circuit. *Energy Procedia* Vol 6, pp 541-549, 2011.
- [4] Amara, Karima, et al. Improved Performance of a PV Solar Panel with Adaptive Neuro Fuzzy Inference System ANFIS based MPPT. *The 7th International Conference on Renewable Energy Research and Applications (ICRERA)*. IEEE, 2018.
- [5] Naguib, Maged F, and Luiz AC Lopes. Harmonics reduction in current source converters using fuzzy logic." *IEEE Transactions on Power Electronics* Vol 25(1), pp 158-167, (2010).
- [6] Alajmi, Bader N., et al. Fuzzy-logic-control approach of a modified hill-climbing method for maximum power point in microgrid standalone photovoltaic system. *IEEE transactions on power electronics* 26.4 (2011): pp 1022-1030.
- [7] Femia, Nicola, et al. Optimization of perturb and observe maximum power point tracking method. *IEEE transactions on power electronics* Vol 20(4), pp 963-973, 2005.
- [8] Al-Atrash, Hussam, Issa Batarseh, and Khalid Rustom. Statistical modeling of DSP-based hill-climbing MPPT algorithms in noisy environments. *Twentieth Annual IEEE Applied Power Electronics Conference and Exposition IEEE*, Vol 3, 2005.
- [9] Safari, Azadeh, and Saad Mekhilef. Simulation and hardware implementation of incremental conductance MPPT with direct control method using cuk converter. *IEEE transactions on industrial electronics* Vol 58(4), pp 1154-1161, 2011.
- [10] Zhang, Jianpo, Tao Wang, and Huijuan Ran. A maximum power point tracking algorithm based on gradient descent method. *Power & Energy Society General Meeting*. IEEE 2009.
- [11] Pradhan, R., and B. Subudhi. A steepest-descent based maximum power point tracking technique for a photovoltaic power system. *The 2nd International Conference on Power, Control and Embedded Systems*. IEEE, 2012.

- [12] Xiao, Weidong, et al. Application of centered differentiation and steepest descent to maximum power point tracking. *IEEE Transactions on Industrial Electronics* Vol 54(5), pp 2539-2549, 2007.
- [13] Verma, Deepak, et al. Comprehensive analysis of maximum power point tracking techniques in solar photovoltaic systems under uniform insolation and partial shaded condition. *Journal of Renewable and Sustainable Energy* Vol 7(4) (2015).
- [14] Femia, Nicola, et al. A technique for improving P&O MPPT performances of double-stage grid-connected photovoltaic systems. *IEEE transactions on industrial electronics* Vol 56(11), pp 4473-4482, 2009.
- [15] Liu, Fangrui, et al. A variable step size INC MPPT method for PV systems. *IEEE Transactions on industrial electronics* Vol 55(7), pp 2622-2628, 2008.
- [16] Teulings, W. J. A., et al. A new maximum power point tracking system. Power Electronics Specialists Conference, PESC'93 Record., 24th Annual IEEE, 1993.
- [17] Koutroulis, Eftichios, Kostas Kalaitzakis, and Nicholas C. Voulgaris. Development of a microcontroller-based, photovoltaic maximum power point tracking control system. *IEEE Transactions on power electronics* Vol 16(1), pp 46-54, 2001.
- [18] Siva Kumar, P., et al. Analysis and enhancement of PV efficiency with incremental conductance MPPT technique under non-linear loading conditions. *Renewable Energy* Vol 81, pp 543-550, 2015.
- [19] Tey, Kok Soon, and Saad Mekhilef. Modified incremental conductance MPPT algorithm to mitigate inaccurate responses under fast-changing solar irradiation level". *Solar Energy* Vol 101, pp 333-342, 2014.
- [20] Necaibia Salah, et al. Implementation of an improved incremental conductance MPPT control based boost converter in photovoltaic applications. *International Journal of Emerging Electric Power Systems* Vol 18(4), 2017.
- [21] Wu, Tasi-Fu, and Yu-Kai Chen. Modeling PWM DC/DC converters out of basic converter units." *IEEE transactions on Power Electronics* Vol 13(5), pp 870-881, 1998.
- [22] Nema, Savita, R. K. Nema, and Gayatri Agnihotri. MATLAB/Simulink based study of photovoltaic cells/modules/array and their experimental verification. *International journal of Energy and Environment* Vol 1(3), pp 487-500, 2010.
- [23] Krithiga, Subramanian, and Nanjappa Gounder Ammasai Gounden. Power electronic configuration for the operation of PV system in combined grid-connected and stand-alone modes. *IET Power Electronics* Vol 7(3), pp 640-647, 2013.
- [24] Lachaize, Jérôme. Etude des stratégies et des structures de commande pour le pilotage des systèmes énergétiques à Pile à Combustible (PAC) destinés à la traction. Diss. 2004.
- [25] Pires, Vitor Fernão, and Jose Fernando A. Silva. Teaching nonlinear modeling, simulation, and control of electronic power converters using MATLAB/SIMULINK. *IEEE Transactions on Education* Vol 45(3), pp 253-261, 2002.
- [26] Buragohain, Mrinal. Adaptive network based fuzzy inference system (ANFIS) as a tool for system identification with special emphasis on training data minimization. Diss.2009.
- [27] Jang, J-SR. "ANFIS: adaptive-network-based fuzzy inference system. *IEEE transactions on systems, man, and cybernetics* Vol 23(3), pp 665-685, 1993.
- [28] Kasabov, Nikola, and Qun Song. DENFIS: dynamic evolving neural-fuzzy inference system and its application for time series prediction. 2002.
- [29] Liu, Fangrui, et al. Comparison of P&O and hill climbing MPPT methods for grid-connected PV converter." *Thr 3rd Conference on Industrial Electronics and Applications, IEEE*, 2008.
- [30] Graditi, G., G. Adinolfi, and A. Del Giudice. Experimental performances of a DMPPT multitopology converter. *International Conference on Renewable Energy Research and Applications (ICRERA). IEEE*, 2015.
- [31] Enany, Mohamed A., Mohamed A. Farhat, and Ahmed Nasr. Modeling and evaluation of main maximum power point tracking algorithms for photovoltaic systems. *Renewable and Sustainable Energy Reviews* Vol 58, pp 1578-1586, 2016.

- [32] Boudia Assam, Sabir Messalti, Abdelghani Hrrag. New Improved Hybrid MPPT Based on Backstepping-sliding Mode for PV System. *Journal Européen des Systèmes Automatisés*. Vol. 52(3), 2019, pp 317-323.
- [33] Safari, A., and Saad Mekhilef. Implementation of incremental conductance method with direct control. *TENCON 2011-2011 IEEE Region 10 Conference*. IEEE, 2011.
- [34] Boukenoui, Rachid, et al. Experimental assessment of Maximum Power Point Tracking methods for photovoltaic systems. *Energy* Vol 132, pp 324-340, 2017.
- [35] Abdelkrim, T., et al. Performance evaluation of a new control scheme of distributed two-stage PV conversion system using three levels voltage source inverter for stand-alone application. *Energy Procedia* Vol 119, pp 270-277, 2017.
- [36] Necaibia, Salah, et al. Practical Implementation of a Proposed MPPT Control Strategy to Mitigate Inaccurate Responses for Photovoltaic Systems. *International Journal on Electrical Engineering & Informatics* Vol 10(4), 2018.



Karima Amara received the magister degree in Electrical Engineering in 2014 from Faculty of Sciences of Tizi Ouzou, Algeria. She is a researcher in the Laboratory of LATAGE, Laboratory of Advanced Technologies of Electrical Engineering (LATAGE), Faculty of Electrical and Computer Engineering, Mouloud Mammeri University (UMMTO), Algeria.



Toufik Bakir received in 2006 his Ph.D. degree in industrial automatics from the University of Claude Bernard-Lyon I, Lyon, France. In 2007, he joined as associate professor the LE2I (Laboratory of Electronics, Computer Science and Image) at the University of Burgundy, Dijon, France. Currently, he is associate professor in ImViA (Image processing and computer Vision) laboratory at the University of Burgundy, Dijon, France. His research interests include dynamic systems, system modeling and control.

Ali MALEK is a research director in Centre de Développement des Energies Renouvelables (CDER, Algiers). His current research interests are photovoltaic (PV) cells, photovoltaic/thermal Air collector and PV systems. He has authored more than 80 scientific papers.



Dalila Hocine was graduated from Mouloud Mammeri University of Tizi-Ouzou (Algeria), and received a PhD in Electronics in 2013. She is now Associate Professor at Mouloud Mammeri University of Tizi-Ouzou and member of the "Semiconductor Materials and Electronic Structures for Photovoltaics" Team of the LATAGE Laboratory. She got her Habilitation for Research Direction (HDR) in 2017. Her current research interests are in the field of nanotechnology, photovoltaic cells, photovoltaic systems, elaboration and characterization of semiconductor materials and solar cells.

She has authored several scientific papers and international communications.



El-Bay Bourennane, 53 years old, is full professor of Electronics at the University of Burgundy, Dijon, France since 2002. He is researcher at the ImViA laboratory (Laboratory of Imaging and computer Vision), Dijon, France. His research interest includes Dynamic reconfigurable systems, Image processing, embedded systems, methodologies and tools for co-modelling and codesign of intensive signal processing specific embedded systems, FPGA design and Real-time systems. He supervised more than 21 PhD thesis. He has written or co-written more than fifty journal papers and more than hundred papers in international conferences on the different topics he has worked on.



Arezki Fekik received the B.Sc., M.Sc., PhD degrees in electrical engineering from Mouloud Mammeri University, Tizi-Ouzou, Algeria, in 2011, 2013 and 2018, respectively. He is currently working at the University of Akli Mohand Oulhadj –Bouira. Arezki is working in the area of power systems, power converters, power electronics and control systems. His research interests include the application of modern control methods (Fuzzy, neurone Petri nets...) to AC/DC converters and Multicellular chopper.



Mustapha Zaouia was born in Tizi Ouzou, Algeria. He received Magister degree from polytechnic School, Algiers, Algeria in 2001 and the PhD degree in Mouloud Mammeri University of Tizi Ouzou Algeria. He is assistant Professor. His research interests the electromagnetic-mechanical modelling, numerical simulation of electromagnetic machines particularly the linear machines and permanent magnet machines applied to the electrical and hybrid vehicles.